JACS
JOURNAL OF THE AMERICAN CHEMICAL SOCIETY
Communication
pubs.acs.org/JACS

Biochemical Characterization of a Eukaryotic Decalin-Forming Diels–Alderase

Li Li,[†,‡] Peiyuan Yu,[§] Man-Cheng Tang,[‡] Yi Zou,[‡] Shu-Shan Gao,[‡] Yiu-Sun Hung,[‡] Muxun Zhao,[‡] Kenji Watanabe,[*,∥] K. N. Houk,[*,‡,§] and Yi Tang[*,‡,§]

[†]Engineering Research Center of Industrial Microbiology (Ministry of Education) and College of Life Sciences, Fujian Normal University, Fuzhou 350117, P. R. China

[‡]Department of Chemical and Biomolecular Engineering and [§]Department of Chemistry and Biochemistry, University of California, Los Angeles, California 90095, United States

[∥]Department of Pharmaceutical Sciences, University of Shizuoka, Shizuoka 422-8526, Japan

Supporting Information

ABSTRACT: The *trans*-decalin structure formed by intramolecular Diels–Alder cycloaddition is widely present among bioactive natural products isolated from fungi. We elucidated the concise three-enzyme biosynthetic pathway of the cytotoxic myceliothermophin and biochemically characterized the Diels–Alderase that catalyzes the formation of *trans*-decalin from an acyclic substrate. Computational studies of the reaction mechanism rationalize both the substrate and stereoselectivity of the enzyme.

Cycloaddition reactions such as intramolecular Diels–Alder (IMDA) reactions are extremely important and versatile synthetic transformations that allow the construction of multicyclic scaffolds with stereocontrol and atom economy.[1] Nature has evolved enzymes to catalyze [4 + 2] reactions in natural product biosynthetic pathways.[2] Especially from bacterial pathways, a few so-called "Diels–Alderases" (DAases) have been discovered and characterized, including those from the spinosyn,[3] solanapyrone,[4] tetronate/tetramate-containing compound,[5] thiopeptide,[6] and abyssomicin[7] pathways. Structural studies suggest that while there are no conserved sequences for DAases, these enzymes provide an active-site environment that accelerates or enables the cycloaddition reactions to occur.[7,8] The diversity of DAases found to date inspires the discovery of additional enzymes that can catalyze such reactions, which can enable genome mining of new natural products that contain structural features derived from cycloaddition reactions.

IMDA reactions are also proposed to occur widely among fungal natural product pathways, in particular those of polyketide and polyketide–nonribosomal peptide natural products.[9] For example, both the *trans*-decalin and isoindolone ring systems found in lovastatin[10] and cytochalasan,[11] respectively, are thought to derive from cycloaddition reactions of acyclic precursors. Decalin-containing fungal polyketides constitute a large class of natural products with a diverse array of biological activities (Figures 1 and S1). Biosynthesis of the acyclic substrates that contain both the dienophile and the diene are proposed to be catalyzed by the iterative functions of the highly reducing polyketide synthases (HR-PKSs). While bioinformatic analysis and genetic evidence have suggested that a class of lipocalin-like enzymes may be involved in the formation of the decalin ring systems of Sch210972[12] and equisetin,[13] no direct biochemical evidence of enzyme-catalyzed IMDA reactions has been described. This is in part due to the inability to capture an acyclic substrate required for activity verification. In this work, we provide biochemical confirmation of DAase activity from a fungal polyketide–nonribosomal peptide biosynthetic pathway using the biosynthesis of myceliothermophin as a model system.

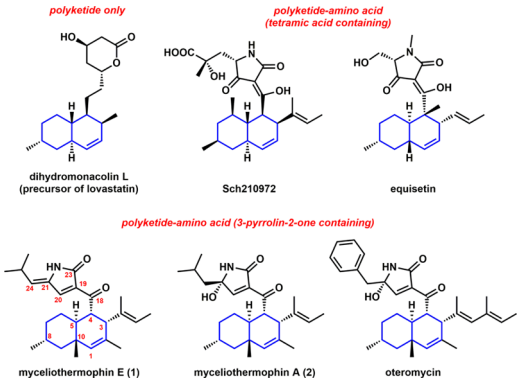

Figure 1. Structures of decalin-containing fungal polyketides and polyketide–amino acid hybrids.

Myceliothermophins, including myceliothermophin E (**1**) and A (**2**), are cytotoxic compounds isolated from the thermophilic fungus *Myceliophthora thermophile* (Figure 1).[14] **1** exhibits IC_{50} values of <100 nM toward a variety of cancer cell lines. Multiple total syntheses of myceliothermophins have been accomplished to establish the absolute stereochemistry as shown in Figure 1.[15,16] Both **1** and **2** contain a trans-fused decalin ring system connected to a conjugated 3-pyrrolin-2-one moiety, with **1** containing an exocyclic methylpropylidene unit derived from leucine at C21, while **2** is substituted with a hydroxyl group at the same position. Despite the wide occurrence of the 3-pyrrolin-2-one ring system in natural products (Figure S1),[17] its formation has not been widely studied. It is proposed to derive from a Knoevenagel condensation between the α-carbon (C19) and a

Received: October 5, 2016
Published: November 28, 2016

DOI: 10.1021/jacs.6b10452
J. Am. Chem. Soc. 2016, 138, 15837–15840

reductively released amino aldehyde (C20). This differs from the tetramic acid rings found in equisetin and Sch210972, which arise from Dieckmann cyclization of aminoacylated polyketides.[18]

To investigate the biosynthetic pathway of **1** and **2**, the genome of the producing organism *M. thermophile* ATCC 42462 was queried for the presence of polyketide synthase−non-ribosomal peptide synthetase (PKS-NRPS)-containing genes. Two PKS-NRPS genes were found, and analysis of the neighboring genes indicated that MYCTH _78013 (named *mycA*), which is near the end of a chromosome, is a likely candidate (Table S2). Immediately adjacent is *mycB* encoding a potential DAase that has sequence homology (36% identity) to CghA, which has been implicated to be involved in the cycloaddition during Sch210972 biosynthesis.[12] A trans-acting enoylreductase (ER) is encoded in *mycC* (Figure 2A). This three-gene cassette is found widely among sequenced fungi (Figure S10). To test the link between the gene cluster and production of **1** and **2**, which are produced by the wild-type strain at yields of 6 and 50 mg/L, respectively (Figure 2B(i); also see Figures S11 and S12 and Tables S3 and S4), the deletion strain Δ*mycA* was generated through gene replacement (Figure S2). LC−MS analysis showed that deletion of *mycA* completely abolished the production of **1** and **2** (Figure 2B(ii)), confirming the involvement of MycA in their biosynthesis. Comparison of the LC−MS traces also revealed the abolishment of **3** and **4**, previously unreported compounds with the same m/z $[M + H]^+$ of 398, which were purified from the wild-type strain in yields of 10 and 16 mg/L (Figure 2C).

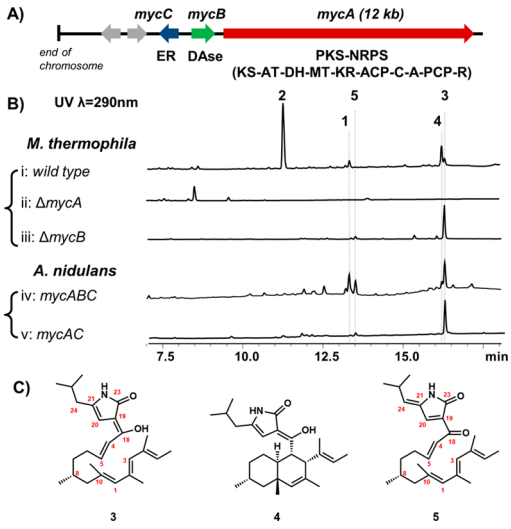

Figure 2. Verification of the myceliothermophin gene cluster. (A) The *myc* cluster encodes the PKS-NRPS MycA (KS, ketosynthase; AT, acyltransferase; DH, dehydratase; MT, methyltransferase; KR, ketoreductase; ACP, acyl carrier protein; C, condensation; A, adenylation; PCP, peptidyl carrier protein; R, reductase), the in trans ER MycC, and the putative DAase MycB. (B) Product profiles of wild-type and single-gene-knockout strains of *M. thermophila* and of *A. nidulans* transformed with combinations of *myc* genes. (C) Structures of metabolites isolated. **3**, **4**, and **5** are assumed to have similar stereochemistries as **1**.

NMR structural characterization showed that **3** is an acyclic polyolefinic compound containing a 4-pyrrolin-2-one moiety that is conjugated with the C18 enol via C19 (Figures 2C, S13, and S20−S24 and Table S5). This is likely the enolized form of the PKS-NRPS/ER product, which contains eight differentially α- and β-functionalized ketide units aminoacylated with leucine and has undergone Knoevenagel condensation (Figure 4). To confirm that **3** is synthesized by PKS-NRPS and ER, we introduced both *mycA* and *mycC* into the heterologous host *Aspergillus nidulans* A1145 (Figure S4). Compared with the untransformed host, *A. nidulans* expressing MycA and MycC showed clear accumulation of a new compound identical to **3** in retention time, UV absorbance, and mass (Figure 2B(v)). This suggests that the *myc* PKS-NRPS and its ER partner are sufficient to form the pyrrolinone moiety, in contrast to previous work with other R-domain-containing fungal PKS-NRPS systems.[19]

On the other hand, **4** is the *trans*-decalin cyclized form of **3** and contains the enolized dienyl pyrrolinone ring (Figures S14 and S25−S30 and Table S6). Thus, **4** represents the potential intermediate that can be oxidized into both **1** and **2**. To examine the role of MycB on the formation of **1**, **2**, and **4** in *M. thermophila*, we generated the Δ*mycB* strain (Figure S3). LC−MS analysis of the metabolites showed that all of these cyclized products were abolished, leaving acyclic **3** as the dominant product (Figure 2B(iii)). Hence, MycB is directly involved in the cycloaddition to form the decalin ring. This was further verified when the entire three-gene cassette *mycABC* was introduced into *A. nidulans* (Figure 2B(iv)). Analysis of the extract showed that compared with *mycAC* alone, introduction of *mycB* led to the emergence of the cyclized product **4** as well as the final metabolite **1**. We could not detect **2** in this strain, suggesting that the stereoselective hydroxylation of C21 is catalyzed by an additional enzyme present only in *M. thermophila*. Analysis of the genes near the *myc* cluster did not reveal any oxygenases that may perform this reaction (Figure S2), and hence, the enzyme may be shared with other pathways in the strain.[20]

In comparing the various extracts analyzed in Figure 2B, we noted a new compound, **5**, that is consistently found in *M. thermophila* Δ*mycB* strain and the transformed *A. nidulans* strains. This compound has m/z $[M + H]^+$ of 396 and λ_{max} = 327 nm (Figure S15), both of which closely resemble those of **1**. Purification of **5** from the Δ*mycB* strain (3 mg/L) followed by NMR characterization (Figures S31−S35) revealed that the new compound is the acyclic form of **1**, which is consistent with its accumulation in the Δ*mycB* and *A. nidulans mycAC* strains. We propose that **5** could be a product of air oxidation of **3**, likely via the same mechanism as for oxidation of **4** to give **1**. We attribute the accumulation of **3** and **5** in the *A. nidulans mycABC* strain to insufficient activity of MycB and/or differences in the redox environment compared with the original producer. Indeed, expressing a second copy of the *mycB* gene led to a decreased amount of **5** and increased amounts of **4** and **1** (Figure S7).

To confirm that MycB is indeed a DAase, *N*-FLAG-tagged recombinant enzyme was heterologously expressed and purified from *Saccharomyces cerevisiae* BJ5464-NpgA (0.2 mg/L) (Figure S5). Either 0.2 mM **3** or **5** was then incubated with 1 μM MycB in Tris buffer (pH 7.4), and the formation of cyclized products was assayed by LC−MS (Figure 3A). No conversion of **3** to **4** was detected under prolonged incubation (**3** degraded after overnight assay), while complete conversion of **5** to **1** was observed in 3 h (Figure 3A,B). Control incubation in the absence of MycB led to degradation of **5** (Figure S6). All of the chromatographic and spectroscopic properties of **1** from the in vitro assay matched those of **1** purified from the in vivo reaction (Figure 2B), showing that MycB can catalyze the IMDA reaction with regio- and stereocontrol. Kinetic measurements showed MycB to have K_M ≈ 75 μM toward **5** and k_{cat} ≈ 0.9 s^{-1} (Figure 3C).

The in vitro results confirmed that MycB can indeed catalyze the DA reaction to convert C18 keto **5** into the cytotoxic natural

DOI: 10.1021/jacs.6b10452
J. Am. Chem. Soc. 2016, 138, 15837−15840

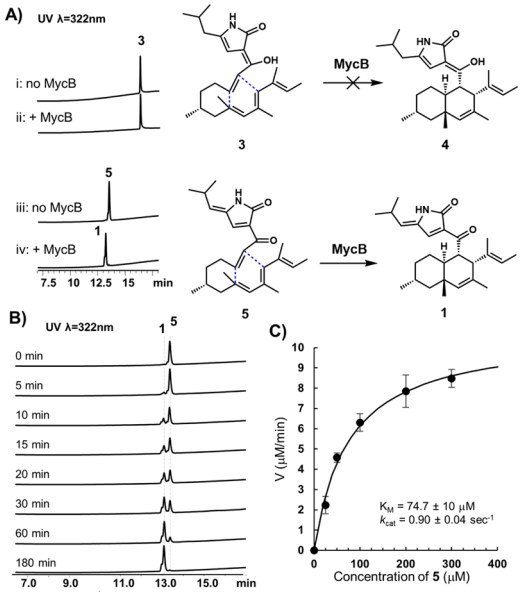

Figure 3. Activity of the DAase MycB. (A) MycB can catalyze the cycloaddition of ketone **5** to give **1** but is not reactive toward enol **3**. (B) Time course analysis of the conversion of **5** to **1**. The starting concentrations of **5** and MycB were 200 and 1 μM, respectively. (C) Saturation kinetics of MycB. Each data point was obtained in triplicate.

product **1**. The failure of MycB to catalyze the conversion of C18 enol **3** into **4**, however, suggests differential reactivity toward the ketone and enol substrates. This difference also leads to a proposed *myc* pathway to account for the isolation of metabolites **1**−**5** (Figure 4). Following MycA-catalyzed construction and release of aminoacyl polyketide aldehyde **6**, Knoevenagel condensation yields the expected ketone **7**. We propose that this ketone is most likely the natural substrate of MycB, leading to the formation of the endo product **8**. The keto-3-pyrrolin-2-one can readily enolize to form the observed **4**. When MycB is inactivated, acyclic **7** can also readily enolize to form **3**, which does not undergo the MycB-catalyzed IMDA reaction. However, both **3** and **4** may undergo spontaneous air oxidation to yield **5** and **1**, respectively (Figure S7). Indeed, when **4** was dissolved in methanol at 37 °C for 16 h, formation of **1** was observed along with equimolar release of H_2O_2 (Figure S8). A proposed oxidation mechanism that involves sequential single-electron reduction of O_2, during which the C18 enol hydrogen is first abstracted, is shown in Figure S9. Significantly (and serendipitously), formation of **5** prevents further tautomerization of the 3-pyrrolin-2-one moiety, resulting in a stable acyclic C18 keto substrate for MycB.

To support the proposed pathway and rationalize the reactivity difference between the C18 keto and enol substrates in the IMDA reaction, we performed density functional theory (DFT) studies on model substrates and products **1′**−**8′**, in which the isobutyl group in **1**−**8** is replaced by a methyl group. The enols **3′** and **4′** were found to be more stable than the corresponding ketones **7′** and **8′**, respectively, with ΔG = −8.0 and −3.5 kcal/mol, respectively (Figure 4), supporting the rapid enolization of **7** into **3** in the absence of MycB.

We then calculated the energetics of the three potential DA reactions shown in Figure 4, starting with either **7′**, **3′**, or **5′**. In each case, the uncatalyzed DA reaction is very slow, with $\Delta G^{\ddagger}_{uncat}$ ≈ 24−25 kcal/mol (Figures S36−S38), corresponding to a rate constant of ~10^{-5} s^{-1} at room temperature according to

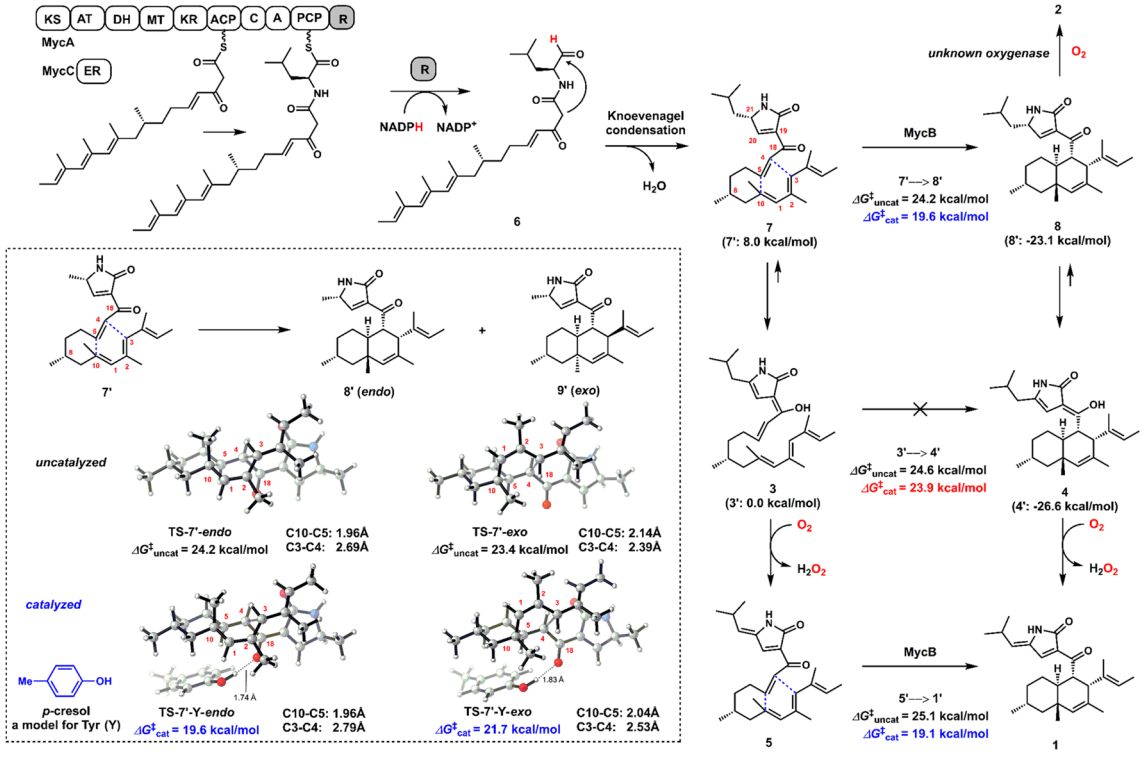

Figure 4. Proposed biosynthetic pathway of **1** based on isolated natural products and biochemical characterization of MycB. DFT analysis were performed on model substrates (**1′**−**8′**) in which the isobutyl group in **1**−**8** is replaced by a methyl group. Calculations were performed at the CPCM(water)/M06-2X/6-311+G(d,p)//M06-2X/6-31G(d) level of theory. The computed free energies of model compounds are shown in parentheses. Calculations of stereoselectivity under uncatalyzed and catalyzed conditions are shown in the dashed box.

DOI: 10.1021/jacs.6b10452
J. Am. Chem. Soc. 2016, 138, 15837−15840

transition state theory. In contrast, the spontaneous DA reaction in the biosynthesis of Sch210972 or equisetin is very fast.[12] The DA reaction of the enol precursor of Sch210972 has a barrier of only 12 kcal/mol because of the additional electron-withdrawing keto group in the tetramate moiety.[12] Interestingly, with **7′**, the uncatalyzed reaction is predicted to produce a mixture of diastereomers (Figure 4, dashed box), with the unobserved cis-fused decalin **9′** being the major isomer, resulting from the lower-energy transition state **TS-7′-*exo***. We propose that a suitable acidic residue in the active site of MycB may accelerate the reaction by lowering the LUMO of the dienophile and stabilizing the transition state through hydrogen bonding to the C18 carbonyl group (in **7** and **5** but not **3**) next to the dienophile. Such a catalytic role for a hydrogen-bond-donating residue is also proposed on the basis of the structures of SpnF and PyrI4.[8] Additionally, because **TS-7′-*endo*** is more asynchronous than **TS7′-*exo***, we envisioned that such a catalyst would stabilize the more polarized endo transition state over the exo transition state.

To test our hypothesis, we used *p*-cresol as a model to probe effects of possible catalytic residues such as a tyrosine in the active site of the enzyme (Figure S39). The catalyzed DA reaction of either **7′** or **5′** is much faster, with $\Delta G^{\ddagger}_{cat} \approx 19$ kcal/mol. This corresponds to a rate constant of ~0.1 s^{-1} at room temperature, which agrees with the experimentally measured rate ($k_{cat} \approx 0.9$ s^{-1}; Figure 3C). Also as predicted, the catalyzed DA reaction of **7′** is computed to be endo-selective to give **8′**, in agreement with the assay results. The H-bond distance in the endo transition state (**TS-7′-Y-*endo***) is shorter than that in the exo transition state (1.74 vs 1.83 Å) because of the more polarized nature of the endo TS. In contrast, the H-bond from cresol to the corresponding enol oxygen in **3′** has only a minimal effect on the rate of its DA reaction, with $\Delta G^{\ddagger}_{cat} = 23.9$ kcal/mol. This is in agreement with the experimental observation that MycB could not catalyze the DA reaction of enol **3**.

In summary, nanomolar cytotoxic **1** is synthesized by a concise three-enzyme pathway. Our findings expand the collection of sought-after DAases from fungi and may lead to the discovery of new decalin-containing natural products using MycB as a signature biosynthetic marker, as shown in Figure S10.

■ ASSOCIATED CONTENT

Supporting Information

The Supporting Information is available free of charge on the ACS Publications website at DOI: 10.1021/jacs.6b10452.

Experimental details and additional data (PDF)

■ AUTHOR INFORMATION

Corresponding Authors

*yitang@ucla.edu
*houk@chem.ucla.edu
*kenji55@u-shizuoka-ken.ac.jp

ORCID

Yi Tang: 0000-0003-1597-0141

Notes

The authors declare no competing financial interest.

■ ACKNOWLEDGMENTS

This work was supported by the NIH (1DP1GM106413 and 1R35GM118056), the NSF (CHE-1361104 to K.N.H.), and the JSPS Program for Advancing Strategic International Networks To Accelerate the Circulation of Talented Researchers (G2604 to K.W.).

■ REFERENCES

(1) Takao, K.-i.; Munakata, R.; Tadano, K.-i. *Chem. Rev.* **2005**, *105*, 4779.
(2) (a) Klas, K.; Tsukamoto, S.; Sherman, D. H.; Williams, R. M. *J. Org. Chem.* **2015**, *80*, 11672. (b) Kim, H. J.; Ruszczycky, M. W.; Liu, H.-w. *Curr. Opin. Chem. Biol.* **2012**, *16*, 124. (c) Zheng, Q.; Tian, Z.; Liu, W. *Curr. Opin. Chem. Biol.* **2016**, *31*, 95.
(3) Kim, H. J.; Ruszczycky, M. W.; Choi, S.-h.; Liu, Y.-n.; Liu, H.-w. *Nature* **2011**, *473*, 109.
(4) Oikawa, H.; Katayama, K.; Suzuki, Y.; Ichihara, A. *J. Chem. Soc., Chem. Commun.* **1995**, *13*, 1321.
(5) (a) Tian, Z.; Sun, P.; Yan, Y.; Wu, Z.; Zheng, Q.; Zhou, S.; Zhang, H.; Yu, F.; Jia, X.; Chen, D.; Mándi, A.; Kurtán, T.; Liu, W. *Nat. Chem. Biol.* **2015**, *11*, 259. (b) Hashimoto, T.; Hashimoto, J.; Teruya, K.; Hirano, T.; Shin-ya, K.; Ikeda, H.; Liu, H.-w.; Nishiyama, M.; Kuzuyama, T. *J. Am. Chem. Soc.* **2015**, *137*, 572.
(6) (a) Wever, W. J.; Bogart, J. W.; Baccile, J. A.; Chan, A. N.; Schroeder, F. C.; Bowers, A. A. *J. Am. Chem. Soc.* **2015**, *137*, 3494. (b) Hudson, G. A.; Zhang, Z.; Tietz, J. I.; Mitchell, D. A.; van der Donk, W. A. *J. Am. Chem. Soc.* **2015**, *137*, 16012.
(7) Byrne, M. J.; Lees, N. R.; Han, L.-C.; van der Kamp, M. W.; Mulholland, A. J.; Stach, J. E. M.; Willis, C. L.; Race, P. R. *J. Am. Chem. Soc.* **2016**, *138*, 6095.
(8) (a) Fage, C. D.; Isiorho, E. A.; Liu, Y.; Wagner, D. T.; Liu, H.-w.; Keatinge-Clay, A. T. *Nat. Chem. Biol.* **2015**, *11*, 256. (b) Zheng, Q.; Guo, Y.; Yang, L.; Zhao, Z.; Wu, Z.; Zhang, H.; Liu, J.; Cheng, X.; Wu, J.; Yang, H.; Jiang, H.; Pan, L.; Liu, W. *Cell Chem. Biol.* **2016**, *23*, 352.
(9) Minami, A.; Oikawa, H. *J. Antibiot.* **2016**, *69*, 500.
(10) Auclair, K.; Sutherland, A.; Kennedy, J.; Witter, D. J.; Van den Heever, J. P.; Hutchinson, C. R.; Vederas, J. C. *J. Am. Chem. Soc.* **2000**, *122*, 11519.
(11) Scherlach, K.; Boettger, D.; Remme, N.; Hertweck, C. *Nat. Prod. Rep.* **2010**, *27*, 869.
(12) Sato, M.; Yagishita, F.; Mino, T.; Uchiyama, N.; Patel, A.; Chooi, Y. H.; Goda, Y.; Xu, W.; Noguchi, H.; Yamamoto, T.; Hotta, K.; Houk, K. N.; Tang, Y.; Watanabe, K. *ChemBioChem* **2015**, *16*, 2294.
(13) Kato, N.; Nogawa, T.; Hirota, H.; Jang, J.-H.; Takahashi, S.; Ahn, J. S.; Osada, H. *Biochem. Biophys. Res. Commun.* **2015**, *460*, 210.
(14) Yang, Y. L.; Lu, C. P.; Chen, M. Y.; Chen, K. Y.; Wu, Y. C.; Wu, S. H. *Chem. - Eur. J.* **2007**, *13*, 6985.
(15) Nicolaou, K.; Shi, L.; Lu, M.; Pattanayak, M. R.; Shah, A. A.; Ioannidou, H. A.; Lamani, M. *Angew. Chem., Int. Ed.* **2014**, *53*, 10970.
(16) Shionozaki, N.; Yamaguchi, T.; Kitano, H.; Tomizawa, M.; Makino, K.; Uchiro, H. *Tetrahedron Lett.* **2012**, *53*, 5167.
(17) (a) Kontnik, R.; Clardy, J. *Org. Lett.* **2008**, *10*, 4149. (b) Suzuki, S.; Hosoe, T.; Nozawa, K.; Kawai, K.-i.; Yaguchi, T.; Udagawa, S.-i. *J. Nat. Prod.* **2000**, *63*, 768. (c) Osterhage, C.; Kaminsky, R.; König, G. M.; Wright, A. D. *J. Org. Chem.* **2000**, *65*, 6412. (d) West, R. R.; Van Ness, J.; Varming, A. M.; Rassing, B.; Biggs, S.; Gasper, S.; McKernan, P. A.; Piggott, J. *J. Antibiot.* **1996**, *49*, 967. (e) Singh, S. B.; Goetz, M. A.; Jones, E. T.; Bills, G. F.; Giacobbe, R. A.; Herranz, L.; Stevens-Miles, S.; Williams, D. L., Jr *J. Org. Chem.* **1995**, *60*, 7040.
(18) (a) Liu, X.; Walsh, C. T. *Biochemistry* **2009**, *48*, 8746. (b) Sims, J. W.; Schmidt, E. W. *J. Am. Chem. Soc.* **2008**, *130*, 11149.
(19) (a) Song, Z.; Bakeer, W.; Marshall, J. W.; Yakasai, A. A.; Khalid, R. M.; Collemare, J.; Skellam, E.; Tharreau, D.; Lebrun, M.-H.; Lazarus, C. M.; Bailey, A. M.; Simpson, T. J.; Cox, R. J. *Chem. Sci.* **2015**, *6*, 4837. (b) Fujii, R.; Minami, A.; Gomi, K.; Oikawa, H. *Tetrahedron Lett.* **2013**, *54*, 2999. (c) Niehaus, E.-M.; Kleigrewe, K.; Wiemann, P.; Studt, L.; Sieber, C. M. K.; Connolly, L. R.; Freitag, M.; Guldener, U.; Tudzynski, B.; Humpf, H.-U. *Chem. Biol.* **2013**, *20*, 1055.
(20) Tsunematsu, Y.; Ishikawa, N.; Wakana, D.; Goda, Y.; Noguchi, H.; Moriya, H.; Hotta, K.; Watanabe, K. *Nat. Chem. Biol.* **2013**, *9*, 818.

DOI: 10.1021/jacs.6b10452
J. Am. Chem. Soc. 2016, 138, 15837−15840